

# 2,5-Bis(1,3-dithiol-2-ylidene)-1,3,4,6-tetrathiapentalene (TTP) derivatives having four long alkylthio chains

Shinya Kimura, Hiroyuki Kurai and Takehiko Mori\*

Department of Organic and Polymeric Materials, Tokyo Institute of Technology, O-okayama, Tokyo 152-8552, Japan

Received 30 October 2001; accepted 10 December 2001

**Abstract**— $\pi$ -Electron donors having four long alkylthio chains,  $\text{TTC}_n$ -TTP (2,5-bis[4,5-bis(alkylthio)-1,3-dithiol-2-ylidene]-1,3,4,6-tetrathiapentalene;  $n=2-5$ ; **1a-d**) have been synthesized. Crystals consisting of the neutral donors show moderately low resistivities ( $6 \times 10^3 - 6 \times 10^7 \Omega \text{ cm}$ ). Origins of the low resistivities are investigated by X-ray analyses;  $\text{TTC}_3$ -TTP (**1b**) displays so-called  $\theta$ -type donor arrangement in contrast to  $\text{TTC}_4$ -TTP (**1c**) with uniform-stacked one, both of which indicate fastener effect. © 2002 Elsevier Science Ltd. All rights reserved.

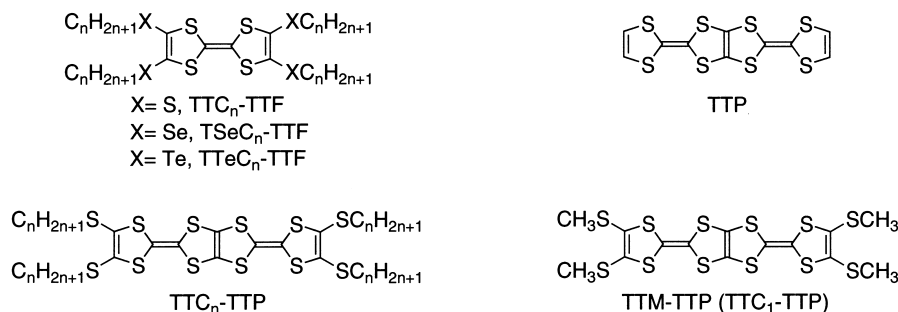
## 1. Introduction

Since the first discovery of organic metals in the 1970s, much effort has been devoted to study organic conductors, not only in the form of charge-transfer complexes but also as single-component crystals. Tetrathiafulvalene (TTF) derivatives with four long alkylthio chains, tetrakis(alkylthio)-TTF ( $\text{TTC}_n$ -TTF,  $n=1-11$ , Scheme 1), have been synthesized and their crystals consisting of the neutral donors have been obtained as single-component organic semiconductors.<sup>1</sup> X-Ray analyses of the crystals have revealed that the donors have dimeric or uniform stacking structure due to the tendency of the alkylthio chains toward aggregation, called ‘fastener effect’. TTF derivatives with much longer chains ( $n > 15$ ) have been synthesized, but no X-ray analysis has been performed.

In addition to the tetrakis(alkylthio)-TTF, tetrakis(alkyl-

seleno)<sup>2</sup> and tetrakis(alkyltelluro)<sup>3</sup> analogs ( $\text{TSeC}_n$ -TTF and  $\text{TTeC}_n$ -TTF, Scheme 1) have been synthesized. It is notable that a single-component crystal of tetrakis(methyltelluro)-TTF ( $\text{TTeC}_1$ -TTF) has high conductivity  $10^{-5} \text{ S cm}^{-1}$  owing to the very strong zigzag  $-\text{Te}-\text{Te}-$  interactions in the crystal structure.<sup>4</sup> The distance between these two Te atoms is 3.644(2) Å, which is much shorter than the van der Waals distance 4.12 Å of Te. The significantly short Te–Te contacts constructing the zigzag chains are called ‘quasi-covalent bonds’.

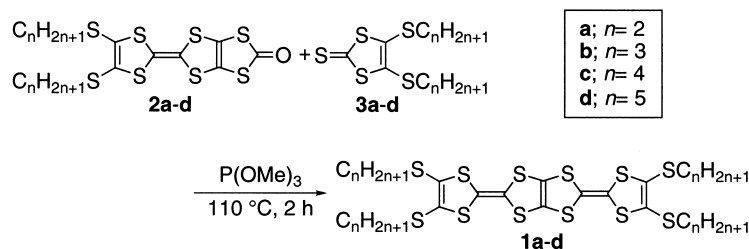
In 1992, a general route to synthesize the extended  $\pi$ -electron donors, having bis-fused TTF structure, 2,5-bis(1,3-dithiol-2-ylidene)-1,3,4,6-tetrathiapentalene (TTP, Scheme 1), was reported.<sup>5</sup> The widely spreading  $\pi$ -system of TTP skeleton seems to be a promising candidate of single-component conductors using the fastener effect. In this line, TTP derivatives with four alkylthio chains are



**Scheme 1.** TTF and TTP type organic donors.

**Keywords:** TTP derivatives; long alkylthio chains; single-component crystal; X-ray analysis; room-temperature resistivity; charge-transfer salts.

\* Corresponding author. Tel.: +81-3-5734-2427; fax: +81-3-5734-3657; e-mail: takehiko@o.cc.titech.ac.jp



Scheme 2. Synthesis of  $\text{TTC}_n\text{-TTP}$ .

designed. Our target molecules,  $\text{TTC}_n\text{-TTP}$  (Scheme 1), are TTP analogs of  $\text{TTC}_n\text{-TTF}$ . On the other hand,  $\text{TTC}_n\text{-TTP}$ 's are long-chain analogs of  $\text{TTC}_1\text{-TTP}$  (TTM-TTP, Scheme 1).<sup>5</sup> These crystals consisting of the neutral donors show relatively low resistivities ( $6 \times 10^3$ – $6 \times 10^7 \Omega \text{ cm}$ ). To examine the fastener effect of the long alkylthio chains in  $\text{TTC}_n\text{-TTP}$ , X-ray analyses of the single crystals of  $\text{TTC}_3\text{-TTP}$  and  $\text{TTC}_4\text{-TTP}$  are carried out.

## 2. Results and discussion

### 2.1. Synthesis

Scheme 2 shows the synthesis of  $\text{TTC}_n\text{-TTP}$  derivatives (**1a–c**). The starting ketones (**2a–d**)<sup>6</sup> and thiones (**3a–d**)<sup>7</sup> were obtained as previously described. The trimethyl phosphite-mediated cross-coupling reactions between **2** and **3** afforded the corresponding TTP derivatives (**1a–d**). In the conventional TTP synthesis, after the coupling reaction, filtration of the product followed by a short column chromatography was used to obtain the pure TTP donors. However, this method is not useful for the present  $\text{TTC}_n\text{-TTP}$ 's because these donors are fairly soluble in trimethyl phosphite, and a considerable part of the product goes to the filtrate. Then trimethyl phosphite was removed in vacuo, and the products were purified by a column chromatography. Succeedingly, the products were recrystallized from toluene to give pure  $\text{TTC}_n\text{-TTP}$ 's in 13–30% yields.

### 2.2. Properties of the donors

Fig. 1 shows the melting points of  $\text{TTC}_n\text{-TTP}$  in comparison

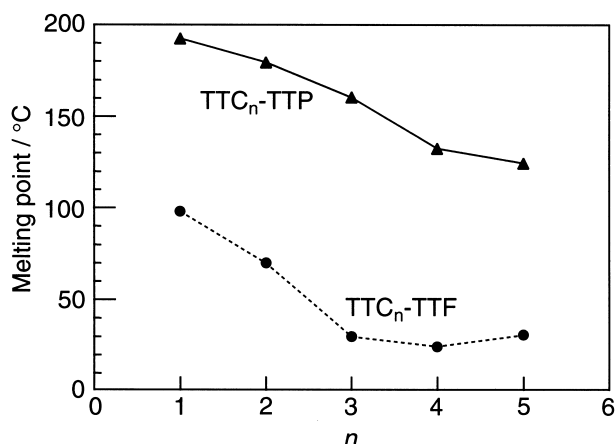


Figure 1. Melting points of  $\text{TTC}_n\text{-TTP}$  and  $\text{TTC}_n\text{-TTF}$  derivatives.

with the  $\text{TTC}_n\text{-TTF}$  series compounds.<sup>7</sup> The melting point of  $\text{TTC}_n\text{-TTF}$  decreases as the length of the alkylthio chains  $n$  increases for  $n < 4$ , but increases after  $n > 4$ . It is noteworthy that the melting point of  $\text{TTC}_4\text{-TTP}$  is so low ( $24.6^\circ\text{C}$ ) that this compound sometimes hardly solidifies at room temperature. By contrast, the melting points of  $\text{TTC}_n\text{-TTP}$  are much higher than those of  $\text{TTC}_n\text{-TTF}$  owing to the large core part, showing no minimum in this  $n$  range.

The redox potentials of  $\text{TTC}_n\text{-TTP}$ 's are summarized in Table 1, together with that of the methylthio analog, TTM-TTP.  $\text{TTC}_2\text{-TTP}$ ,  $\text{TTC}_3\text{-TTP}$ , and  $\text{TTC}_5\text{-TTP}$  show four reversible redox couples, like TTM-TTP. Although the fourth redox couples of  $\text{TTC}_4\text{-TTP}$  have not been observed clearly, the TTP moiety can be oxidized up to 4+. The values are almost the same as those of TTM-TTP.

Table 1. Redox potentials of  $\text{TTC}_n\text{-TTP}$  derivatives (V)

n	Compound	$E_1$	$E_2$	$E_3$	$E_4$	$E_2 - E_1$
1	TTM-TTP	+0.49	+0.69	+1.00	+1.09	0.20
2	<b>1a</b>	+0.46	+0.69	+0.99	+1.11	0.23
3	<b>1b</b>	+0.46	+0.69	+1.00	+1.15	0.23
4	<b>1c</b>	+0.44	+0.66	+1.02	–	0.22
5	<b>1d</b>	+0.47	+0.68	+1.00	+1.16	0.21

vs. Ag/AgCl in  $\text{Bu}_4\text{NPF}_6/\text{PhCN}$ .

### 2.3. Room-temperature resistivities

Single-component crystals of the newly synthesized donors are obtained as red or orange crystals by slow evaporation of dichloromethane–hexane and dichloromethane–methanol solutions. The resistivities of the crystals are measured by the two-probe method at room temperature. All compounds show remarkably low resistivities: ca.  $6 \times 10^7$  for  $\text{TTC}_2\text{-TTP}$ ,  $5 \times 10^5$  for  $\text{TTC}_3\text{-TTP}$ ,  $6 \times 10^3$  for  $\text{TTC}_4\text{-TTP}$ , and  $4 \times 10^5 \Omega \text{ cm}$  for  $\text{TTC}_5\text{-TTP}$ . As shown in Table 2, these values are two or three orders smaller than those of  $\text{TTC}_n\text{-TTF}$ 's (ca.  $10^6$ – $10^{10} \Omega \text{ cm}$ ) with the same  $n$  region.<sup>1,3</sup> This may be associated with the molecular packing preferable to

Table 2. Room-temperature resistivities of  $\text{TTC}_n\text{-TTP}$  and  $\text{TTC}_n\text{-TTF}$  derivatives ( $\Omega \text{ cm}$ )

n	$\text{TTC}_n\text{-TTP}$	$\text{TTC}_n\text{-TTF}$
2	$6 \times 10^7$	$1 \times 10^{10}$
3	$5 \times 10^5$	$1 \times 10^8$
4	$6 \times 10^3$	$6 \times 10^6$
5	$4 \times 10^5$	$6 \times 10^7$

**Table 3.** Crystallographic data

	TTC <sub>3</sub> -TTP	TTC <sub>4</sub> -TTP
Chemical formula	C <sub>22</sub> H <sub>28</sub> S <sub>12</sub>	C <sub>26</sub> H <sub>36</sub> S <sub>12</sub>
Formula weight	677.18	733.29
Shape	Red plate	Red plate
Crystal system	Orthorhombic	Triclinic
Space group	<i>Pbca</i>	<i>P</i> -1
<i>a</i> (Å)	10.611(5)	8.956(4)
<i>b</i> (Å)	31.83(1)	18.300(9)
<i>c</i> (Å)	9.110(6)	5.325(3)
$\alpha$ (°)	90	98.41(4)
$\beta$ (°)	90	99.55(4)
$\gamma$ (°)	90	80.53(4)
<i>V</i> (Å <sup>3</sup> )	3077(2)	849.1(7)
<i>Z</i>	4	1
<i>D</i> <sub>calcd</sub> (g cm <sup>-3</sup> )	1.462	1.434
Temperature (K)	300	300
<i>R</i> / <i>R</i> <sub>w</sub>	0.038/0.041	0.047/0.049
Reflections used	1594	1698

carrier transport, demonstrating the enhanced fastener effect in the TTP series. Recently, a neutral metal complex, which is also derived from the synthetic route to TTP, is reported to show even metallic conductivity.<sup>8</sup>

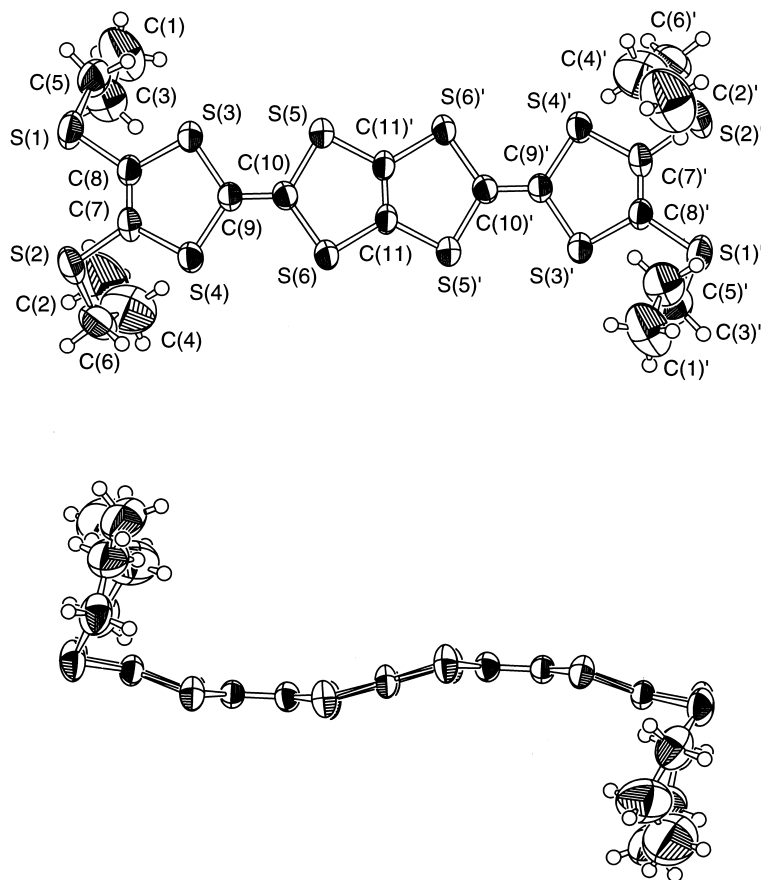
#### 2.4. X-ray analysis

To discuss the low resistivities of TTC<sub>*n*</sub>-TTP's from the viewpoint of crystal structure, X-ray analyses are carried out. Among the crystals obtained, those of TTC<sub>3</sub>-TTP and

TTC<sub>4</sub>-TTP have sufficient quality for X-ray analysis. The crystal data are summarized in Table 3.

The atomic numbering scheme of neutral TTC<sub>3</sub>-TTP is shown in Fig. 2. The TTP skeleton, which is located on an inversion center, bends like 'S' shape. The four propylthio chains extend out of the molecular plane with a tilt to the inner direction. Fig. 3(a) shows that the donor arrangement is  $\theta$ -type<sup>9</sup> with the dihedral angle of 131°, where the donors make uniform pseudo-stacks along the *a* axis.  $\theta$ -Type donor arrangement has not been found in neutral TTC<sub>*n*</sub>-TTF, many of which have  $\beta''$ -like structures.<sup>1,10</sup> The overlap integrals of HOMO are  $a=5.00$ ,  $p=2.91$ , and  $q=3.12 \times 10^{-3}$  (Fig. 3(a)). The values of the intracolumnar overlap  $p$  and  $q$  are small in accordance with the large dihedral angle. As shown in Fig. 3(b), the donors in the alternating donor sheets are tilted in the opposite directions. The TTP parts are separated by non-conducting domains consisting of the propylthio chains, so that no interaction exists between the TTP units of the adjacent donor sheets. In the pseudo-columns, the interplane distance is 4.33 Å, and the slip distances along the donor long and short axes are 8.53, and 4.59 Å, respectively (Fig. 3(c)). In this structure, the slip distance along the molecular short axis is very large in comparison with the typical ring-over-atom structure (1.6 Å). In addition, the long axis slip is anomalously large as well. In spite of these unusually large slips, the donors maintain conducting paths realizing the low resistivity.

The atomic numbering scheme of neutral TTC<sub>4</sub>-TTP is

**Figure 2.** ORTEP drawing and atomic numbering scheme of TTC<sub>3</sub>-TTP.

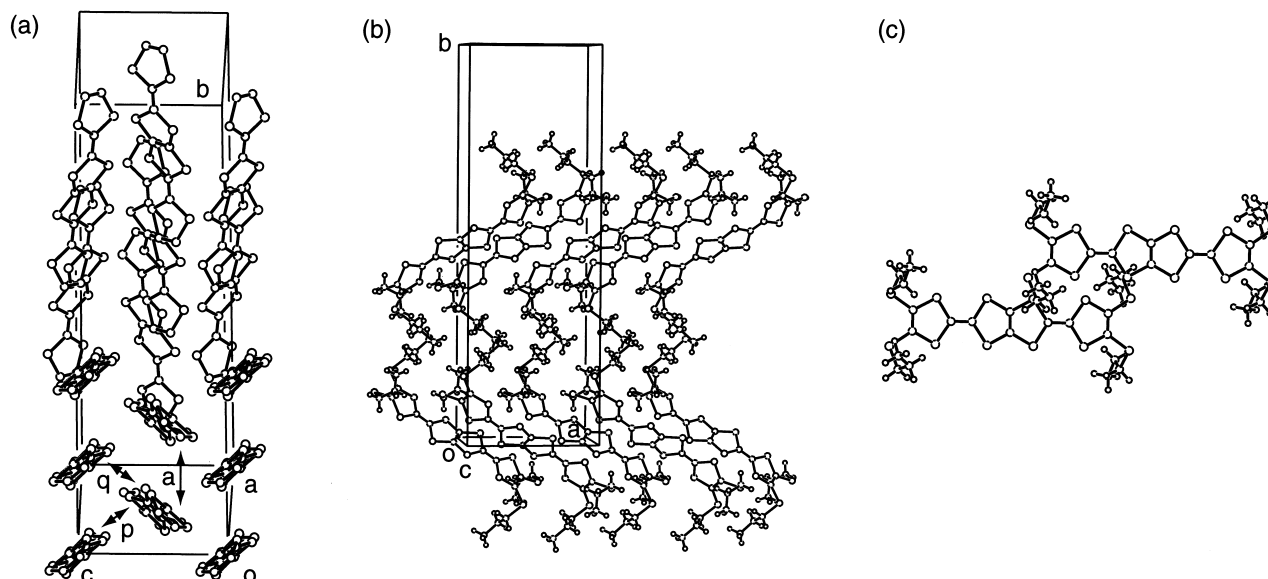


**Figure 3.** Crystal structure of  $\text{TTC}_3\text{-TTP}$ . (a) View along the molecular long axis (propylthio chains are omitted for the sake of clarity), (b) projection onto the  $ab$  plane, and (c) overlap mode of the intrastack donors.

shown in Fig. 4. A TTP donor is located on an inversion center. Unlike  $\text{TTC}_3\text{-TTP}$ , the TTP moiety is almost flat and four alkylthio chains are standing nearly perpendicular to the TTP plane. As shown in Fig. 5(a), the donors stack uniformly along the  $c$  axis, and the TTP sheets are separated by the alkyl domains (Fig. 5(b)). The donor molecular structure and the arrangement in the crystal are similar to those of

$\text{TTM-TTP}$  and many of  $\text{TTC}_n\text{-TTF}$ 's with long alkylthio chains. According to Ref. 1(c), this type of conformation is categorized as Chair III. The overlap integrals are  $c=1.14$  and  $p=2.57 \times 10^{-3}$ . The stacking manner in the columns is shown in Fig. 5(c). The donors in the chain slip along the donor long axis ( $3.57 \text{ \AA}$ ) and along the short axis ( $1.83 \text{ \AA}$ ), so that the donor arrangement is classified as  $\beta''$ -phase. A

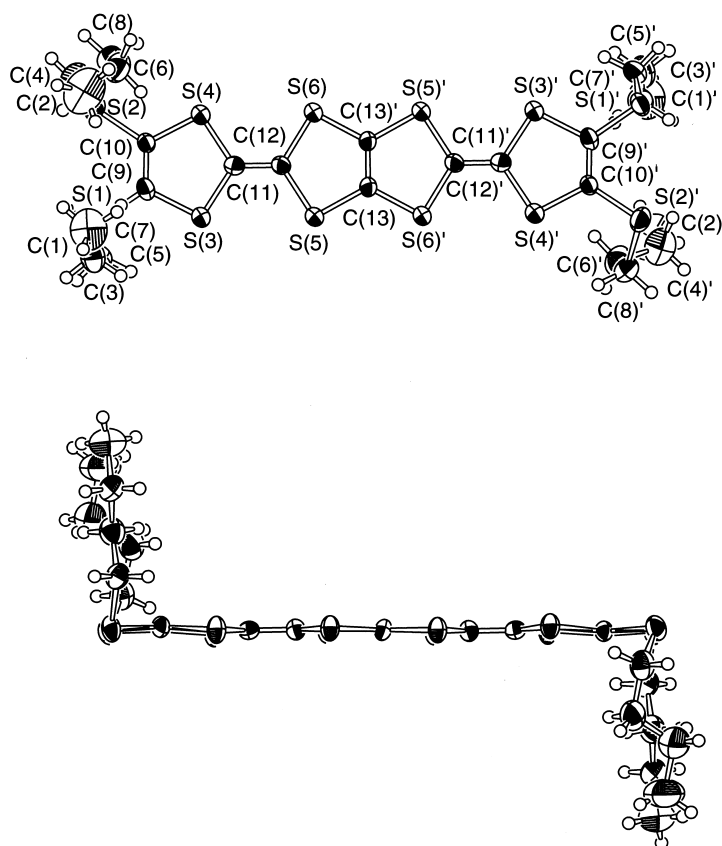


**Figure 4.** ORTEP drawing and atomic numbering scheme of  $\text{TTC}_4\text{-TTP}$ .

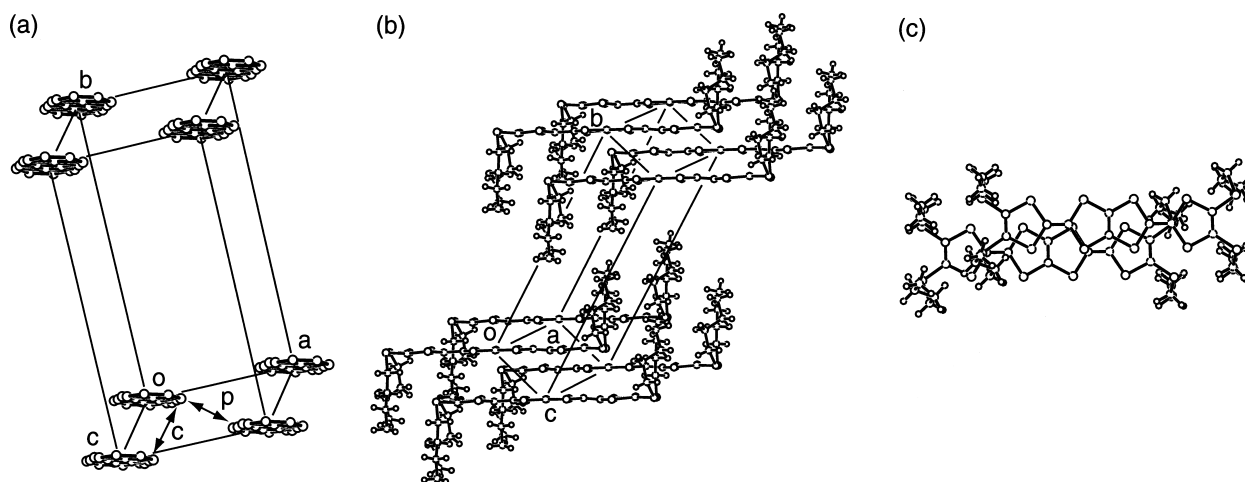


**Figure 5.** Crystal structure of  $\text{TTC}_4\text{-TTP}$ . (a) View along the molecular long axis (buthylthio chains are omitted for the sake of clarity), (b) along the short axis, and (c) overlap mode of the intrastack donors.

similar donor overlap pattern has been also observed in neutral  $\text{TTC}_4\text{-TTF}$  (slip along the long and short axis: 3.81 and 1.63 Å). The lattice constants of  $\text{TTC}_4\text{-TTP}$ , except for that along the molecular long axis are very close to those of  $\text{TTC}_4\text{-TTF}$ ; compare  $a=8.956(4)$ ,  $c=5.325(3)$  Å, and  $\beta=99.55(4)^\circ$  for  $\text{TTC}_4\text{-TTP}$ , with  $a=9.021(1)$ ,  $c=5.397(4)$  Å, and  $\beta=94.05(6)^\circ$  for  $\text{TTC}_4\text{-TTF}$ . Although the  $\text{TTC}_4\text{-TTF}$  and  $\text{TTC}_4\text{-TTP}$  have different  $\pi$ -skeletons, the two-dimensional packing patterns of the core parts are essentially the same. In addition, the interplanar distances of  $\text{TTC}_4\text{-TTF}$  and  $\text{TTC}_4\text{-TTP}$  are not so different; 3.43 and 3.50 Å, respectively. It indicates that the tight donor stacking of  $\text{TTC}_4\text{-TTF}$  does not change so much even after the TTF skeleton is replaced by a TTP skeleton. Consequently, the crystal of  $\text{TTC}_4\text{-TTP}$  show such a low resistivity.

## 2.5. Charge-transfer complexes

Charge-transfer complexes of  $\text{TTC}_2\text{-TTP}$  with  $\text{BF}_4$  and  $\text{ClO}_4$  are obtained in the form of black needles by electrochemical oxidation in 1,2-dichloroethane in the presence of the corresponding tetrabutylammonium salts. From the elemental analysis of the  $\text{ClO}_4$  salt, the donor: acceptor ratio is found to be 2:1, but that of the  $\text{BF}_4$  salt is not determined. Both salts ( $\sigma_\pi=34 \text{ S cm}^{-1}$  for the  $\text{BF}_4$  salt and  $2 \text{ S cm}^{-1}$  for the  $\text{ClO}_4$  salt) have almost flat temperature dependence of the conductivity down to 250 K, and the conductivity gradually decreases below this temperature. However, we could not analyze the crystal structures. Although attempts to prepare charge-transfer complexes of other  $\text{TTC}_n\text{-TTP}$ 's are carried out, no salts are obtained.

## 3. Conclusions

TTP derivatives with four long alkylthio chains,  $\text{TTC}_n\text{-TTP}$  ( $n=2-5$ ) are prepared. All the single crystals consisting of the neutral donors show quite a low resistivities ranging from  $6 \times 10^3$  to  $6 \times 10^7$ . The crystal structures of neutral  $\text{TTC}_3\text{-TTP}$  and  $\text{TTC}_4\text{-TTP}$  indicate that the low resistivities result from aggregation of the aliphatic moieties, called fastener effect. The  $\theta$ -phase crystal structure of neutral  $\text{TTC}_3\text{-TTP}$  seems to be quite different from  $\beta''$ -structure

of neutral  $\text{TTC}_4\text{-TTP}$ , but these two phases have the same ring-over-atom type overlap pattern. The  $\beta''$ -phase is generated by rotating the molecules of every other column of the  $\theta$ -phase.<sup>10</sup> Furthermore, the crystal of neutral  $\text{TTC}_1\text{-TTP}$  ( $\text{TTC}_1\text{-TTP}$ ) has the same  $\beta''$ -structure with slip distances along the donor long (3.47 Å) and short (1.51 Å) axes. By contrast,  $\beta''$ -structure is very rare in charge-transfer complexes of TTP.<sup>11</sup> All the crystals of neutral TTP ( $\text{TTC}_1\text{-TTP}$ ,  $\text{TTC}_3\text{-TTP}$ , and  $\text{TTC}_4\text{-TTP}$ ) so far analyzed have ring-over-atom donor overlaps, although only the  $\text{TTC}_3\text{-TTP}$  has an exceptional  $\theta$ -type arrangement. This strong tendency to form the ring-over-atom overlap is interpreted in view of the large closed shell repulsion of the extended  $\pi$ -skeleton, with avoiding the repulsion by sliding the molecule along the molecular short axis. On the other hand, charge-transfer complexes obtained from TTP derivatives prefer  $\beta$ -type uniform structures. When some electron of HOMO is removed in the charge-transfer salts, bonding character between the HOMO's of the adjacent molecules emerges. This tends to give rise to  $\beta$ -type structure with relatively large  $\pi$ - $\pi$  intermolecular overlaps. Like this, correlation and difference between structures of single-component and charge-transfer crystals are important from the viewpoint of exploring single-component donors showing much lower resistivities.

## 4. Experimental

### 4.1. General data

Trimethyl phosphite was distilled under argon by fractional distillation. Melting points were determined with a Yanaco MP micro melting point apparatus. NMR spectra were obtained with a JEOL JNM-AL300 spectrometer. CV spectra were measured on a Yanaco VMA-010 spectrometer. Microanalyses were performed at Microanalytical Laboratory, Tokyo Institute of Technology. IR spectra were recorded on a SHIMADZU FTIR-8000 spectrometer.

**4.1.1.  $\text{TTC}_2\text{-TTP}$  (1a).** Ketone **2a** (181 mg, 0.436 mmol) and thione **3a** (287 mg, 1.13 mmol) were cross-coupled in excess trimethyl phosphite (7 ml) at  $110^\circ\text{C}$  under argon

atmosphere for 2 h. After trimethyl phosphite was evaporated in vacuo, the residue was chromatographed on silica gel with CS<sub>2</sub> as the eluent. Recrystallization from toluene afforded **1a** (52.0 mg, 19.2%) as a red solid. Mp 179–180°C; IR (KBr)  $\nu_{\max}$  1443, 1416, 961, 885, 760 cm<sup>-1</sup>; <sup>1</sup>H NMR (300 MHz, CDCl<sub>3</sub>)  $\delta$ (ppm): 1.31 (t, 12H, *J*=7.4 Hz), 2.83 (q, 8H, *J*=7.4 Hz); Anal. calcd for C<sub>18</sub>H<sub>20</sub>S<sub>12</sub>·0.5H<sub>2</sub>O: C, 33.70; H, 3.05; S, 63.24. Found: C, 33.90; H, 3.01; S, 62.10%. Compounds **1b** and **1c** were prepared similarly.

**4.1.2. TTC<sub>3</sub>-TTP (1b).** 13.0% yield; red solid; mp 160–161°C; IR (KBr)  $\nu_{\max}$  1455, 1414, 959, 891, 764 cm<sup>-1</sup>; <sup>1</sup>H NMR (300 MHz, CDCl<sub>3</sub>)  $\delta$ (ppm): 1.02 (t, 12H, *J*=7.4 Hz), 1.66 (m, 8H), 2.79 (t, 8H, *J*=7.2 Hz); Anal. calcd for C<sub>22</sub>H<sub>28</sub>S<sub>12</sub>·0.5CS<sub>2</sub>: C, 37.77; H, 3.95; S, 58.28%. Found: C, 38.30; H, 3.92; S, 58.07%.

**4.1.3. TTC<sub>4</sub>-TTP (1c).** 27.9% yield; red solid; mp 132–133°C; IR (KBr)  $\nu_{\max}$  1460, 1416, 961, 889, 766 cm<sup>-1</sup>; <sup>1</sup>H NMR (300 MHz, CDCl<sub>3</sub>)  $\delta$  (ppm): 0.93 (t, 12H, *J*=7.2 Hz), 1.43 (m, 8H), 1.60 (m, 8H), 2.82 (t, 8H, *J*=7.2 Hz); Anal. calcd for C<sub>26</sub>H<sub>36</sub>S<sub>12</sub>·0.5CS<sub>2</sub>: C, 41.25; H, 4.70; S, 54.04%. Found: C, 41.78; H, 4.07; S, 51.47%.

**4.1.4. TTC<sub>5</sub>-TTP (1d).** 29.7% yield; red solid; mp 124–125°C; IR (KBr);  $\nu_{\max}$  1458, 1418, 960, 890, 766 cm<sup>-1</sup>; <sup>1</sup>H NMR (300 MHz, CDCl<sub>3</sub>)  $\delta$  (ppm): 0.90 (t, 12H, *J*=7.2 Hz), 1.38 (m, 16H), 1.62 (m, 8H), 2.81 (t, 8H, *J*=7.4 Hz); Anal. calcd for C<sub>30</sub>H<sub>44</sub>S<sub>12</sub>: C, 45.65; H, 5.62; S, 48.74%. Found: C, 44.93; H, 5.49; S, 47.57%.

## 4.2. X-Ray analysis

The data were collected on a Rigaku AFC7R diffractometer with graphite monochromated Mo K $\alpha$  radiation and a rotating anode generator using the  $\omega$  scan technique to a maximum  $2\theta$  of 60°. The structure was solved by the direct method and refined by full-matrix least-squares analysis (anisotropic for non-hydrogen atoms). All calculations

were performed using the teXsan crystallographic software package of Molecular Structure Corporation. Atomic coordinates, bond distances and angles, and thermal parameters have been deposited at the Cambridge Crystallographic Data Center (No. 172794 and 172795).

## References

1. (a) Inokuchi, H.; Saito, G.; Wu, P.; Seki, K.; Tang, T. B.; Mori, T.; Imaeda, K.; Enoki, T.; Higuchi, Y.; Inaka, K.; Yasuoka, N. *Chem. Lett.* **1986**, 1263–1266. (b) Nakano, C.; Mori, T.; Imaeda, K.; Yasuoka, N.; Maruyama, Y.; Inokuchi, H.; Iwasawa, N.; Saito, G. *Bull. Chem. Soc. Jpn.* **1992**, *65*, 1878–1883. (c) Nakano, C.; Mori, T.; Imaeda, K.; Yasuoka, N.; Maruyama, Y.; Inokuchi, H.; Iwasawa, N.; Saito, G. *Bull. Chem. Soc. Jpn.* **1992**, *65*, 2086–2092.
2. Wang, P.; Mori, T.; Nakano, C.; Maruyama, Y.; Inokuchi, H.; Iwasawa, N.; Yamochi, H.; Urayama, H.; Saito, G. *Bull. Chem. Soc. Jpn.* **1988**, *61*, 3455–3459.
3. Imaeda, K.; Enoki, T.; Shi, Z.; Wu, P.; Okada, N.; Yamochi, H.; Saito, G.; Inokuchi, H. *Bull. Chem. Soc. Jpn.* **1987**, *60*, 3163–3167.
4. Inokuchi, H.; Imaeda, K.; Enoki, T.; Mori, T.; Maruyama, Y.; Saito, G.; Okada, N.; Yamochi, H.; Seki, K.; Higuchi, Y.; Yasuoka, N. *Nature* **1987**, *329*, 39–40.
5. Misaki, Y.; Nishikawa, H.; Kawakami, K.; Koyanagi, S.; Yamabe, T.; Shiro, M. *Chem. Lett.* **1992**, 2321–2324.
6. Kimura, S.; Kurai, H.; Mori, T. *Mol. Cryst. Liq. Cryst.* in press.
7. Wu, P.; Saito, G.; Imaeda, K.; Shi, Z.; Mori, T.; Enoki, T.; Inokuchi, H. *Chem. Lett.* **1986**, 441–444.
8. Tanaka, H.; Okano, Y.; Kobayashi, H.; Suzuki, W.; Kobayashi, A. *Science* **2001**, *291*, 285–287.
9. Mori, T.; Mori, H.; Tanaka, S. *Bull. Chem. Soc. Jpn.* **1999**, *72*, 179–197.
10. Mori, T. *Bull. Chem. Soc. Jpn.* **1998**, *71*, 2509–2526.
11. Mori, T.; Inokuchi, H.; Misaki, Y.; Nishikawa, H.; Yamabe, T.; Mori, H.; Tanaka, S. *Chem. Lett.* **1993**, 2085–2088.